ACCOUNTS of chemical research

Article

pubs.acs.org/accounts

Toward the Synthesis of More Reactive $S = 2$ Non-Heme Oxoiron(IV) Complexes

Published as part of the Accounts of Chemical Research special issue "Synthesis in Biological Inorganic Chemistry".

Mayank Puri and Lawrence Que, Jr.*

Department of Chemistry and Center for Metals in Biocatalysis, University of Minnesota, Minneapolis, Minnesota 55455, United States

CONSPECTUS: 2003 marked a banner year in the bioinorganic chemistry of mononuclear non-heme iron enzymes. The first non-heme oxoiron(IV) intermediate (called ***J***) was trapped and characterized by Bollinger and Krebs in the catalytic cycle of taurine dioxygenase (TauD), and the first crystal structure of a synthetic non-heme oxoiron(IV) complex was reported by Münck, Nam, and Que. These results stimulated inorganic chemists to synthesize related oxoiron(IV) complexes to shed light on the electronic structures and spectroscopic properties of these novel intermediates and gain mechanistic insights into their function in biology. All of the biological oxoiron(IV) intermediates discovered since 2003 have an $S = 2$ ground spin state, while over 90% of the 60 or so synthetic oxoiron(IV) complexes reported to date have an $S = 1$ ground spin state. This difference in electronic structure has fueled an interest to more accurately model these enzymatic intermediates and synthesize $S = 2$ oxoiron(IV) complexes.

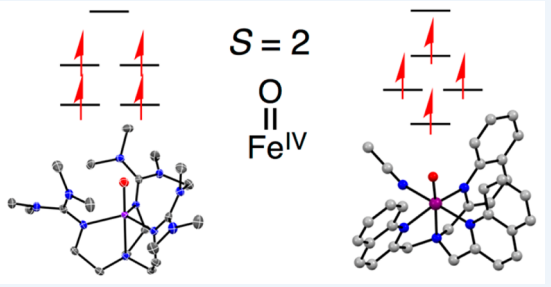

This Account follows up on a previous Account (*Acc. Chem. Res.* **2007**, *40*, 493) that provided a perspective on the early developments in this field up to 2007 and details our group's efforts in the development of synthetic strategies to obtain oxoiron(IV) complexes with an $S = 2$ ground state. Upon inspection of a qualitative d-orbital splitting diagram for a d^4 metal−oxo center, it becomes evident that the key to achieving an $S = 2$ ground state is to decrease the energy gap between the $d_{x^2-y^2}$ and d_{xy} orbitals. Described below are two different synthetic strategies we used to accomplish this goal.

The first strategy took advantage of the realization that the $d_{x^2-y^2}$ and d_{xy} orbitals become degenerate in a C_3-symmetric ligand environment. Thus, by employing bulky tripodal ligands, trigonal-bipyramidal $S = 2$ oxoiron(IV) complexes were obtained. However, substrate access to the oxoiron(IV) center was hindered by the bulky ligands, and the complexes showed limited ability to cleave substrate C−H bonds. The second strategy entailed introducing weaker-field equatorial ligands in six-coordinate oxoiron(IV) complexes to decrease the $d_{x^2-y^2}/d_{xy}$ energy gap to the point where the $S = 2$ ground state is favored. These pseudo-octahedral $S = 2$ oxoiron(IV) complexes exhibit high H-atom transfer reactivity relative to their $S = 1$ counterparts and shed light on the role that the spin state may play in these reactions. Among these complexes is a highly reactive species that to date represents the closest electronic and functional model of the enzymatic intermediate, TauD-***J***.

1. INTRODUCTION

Non-heme iron enzymes carry out critical oxidative transformations in biology.[1] These enzymes activate dioxygen, with the aid of a two-electron sacrificial reductant, to generate a highly reactive oxoiron(IV) species, which is proposed to be the active intermediate in the oxidation of a number of important biomolecules. Oxoiron(IV) intermediates have been elegantly trapped and characterized by the efforts of Krebs and Bollinger in a number of different enzymes,[2] the first of which was taurine dioxygenase (TauD) in 2003.[3,4] The enzymatic oxoiron(IV) intermediate, TauD-***J***, has an $S = 2$ ground spin state with an isomer shift of 0.30 mm/s. The high-spin state of TauD-***J*** has been rationalized by the presence of weak-field ligands, such as histidines and carboxylates, that support the $Fe^{IV}(O)$ center. Since 2003, oxoiron(IV) intermediates in two more classes of non-heme iron enzymes have been trapped and characterized, all of which demonstrate $S = 2$ ground states with isomer shifts in the range of 0.22−0.30 mm/s (Table 1).[2,5]

Also in 2003, we reported the first structurally characterized synthetic oxoiron(IV) complex, $[Fe^{IV}(O)(TMC)(MeCN)]^{2+}$.[6] However, unlike TauD-***J***, $[Fe^{IV}(O)(TMC)(MeCN)]^{2+}$ has an $S = 1$ ground spin state, and its Mossbauer parameters are notably different, with an isomer shift of 0.17 mm/s. In the years since, over 60 additional synthetic oxoiron(IV) species have been reported, with more than 90% of them characterized as having an $S = 1$ ground state.[5] The initial investigations of these new $S = 1$ oxoiron(IV) complexes were discussed in a 2007 Account by one of us.[7] At the time, the only reported $S = 2$ oxoiron(IV) complex was $[Fe^{IV}(O)(OH_2)_5]^{2+}$ (**1**) (Figure 1), characterized by Bakac,[8] in which the oxoiron(IV) center is

Received: May 6, 2015
Published: July 15, 2015

DOI: 10.1021/acs.accounts.5b00244
Acc. Chem. Res. 2015, 48, 2443−2452

Table 1. Spectroscopic Signatures of Selected S = 1 and S = 2 Oxoiron(IV) Species

complex	S	near-IR bands (nm)	δ (mm/s)	ΔE_Q (mm/s)	D (cm^{-1})	ref(s)
$[Fe^{IV}(O)(TMC)(MeCN)]^{2+}$	1	824	0.17	1.24	27	6, 59
$[Fe^{IV}(O)(N4Py)]^{2+}$	1	695	−0.04	0.93	22	60
$[Fe^{IV}(O)(OH_2)_5]^{2+}$ (**1**)	2		0.38	0.33	9.7(7)	8
$[Fe^{IV}(O)(TMG_3tren)]^{2+}$ (**2**)	2	825	0.09	−0.29	5.0(5)	15
$[Fe^{IV}(O)(TMG_2dien)(X)]^{+/2+}$ (**3-X**)						
X = MeCN	2	724, 805	0.08	0.58	4.5(5)	17
X = Cl	2	745, 803	0.08	0.41	4.0(5)	
X = N_3	2	827	0.12	−0.30	4.6(5)	
$[Fe^{IV}(O)(H_3buea)]^{1-}$ (**4**)	2	808	0.02	0.43	4.0(5)	12
$[Fe^{IV}(O)(tpa^{Ph})]^{1-}$ (**5**)	2	∼900	0.09	0.51	4.3	20
$[Fe^{IV}(O)(TPA^*)(MeCN)]^{2+}$ (**11**)	1		0.01	0.95		61
$[(HO)(L)\ Fe^{IV}{-}O{-}Fe^{IV}(O)(L)]^{3+}$ (L = TPA*) (**10**)	1		−0.03	0.92		61
$[(TPA^*)_2Fe^{IV}{}_2(\mu\text{-}O)_2]^{4+}$	1		−0.03	2.04		62
$[(TPA^*)_2Fe^{III}Fe^{IV}(\mu\text{-}O)_2]^{3+}$ (**6**)	1		0.11	0.44		62
$[(HO)(L)Fe^{III}{-}O{-}Fe^{IV}(O)(L)]^{2+}$ (L = TPA*) (**7**)	2		0.09	−0.40		24
$[(F)(L)Fe^{III}{-}O{-}Fe^{IV}(O)(L)]^{2+}$ (L = TPA*) (**8**)	2		0.10	0.60		25
$[(H_2O)(L)\ Fe^{III}{-}O{-}Fe^{IV}(O)(L)]^{3+}$ (L = $6Me_3$TPA)	2		0.10	1.14		38, 39
$[(H_2O)(L)\ Fe^{III}{-}O{-}Fe^{IV}(O)(L)]^{3+}$ (L = 6MeTPA)	2		0.08	0.5		40
$[Fe^{IV}(O)(TPA)(MeCN)]^{2+}$	1	724	0.01	0.92	28(2)	63
$[Fe^{IV}(O)(6MeTPA)(MeCN)]^{2+}$ (**12**)	1	770				42
$[Fe^{IV}(O)(QBPA)(MeCN)]^{2+}$ (**13**)	1	770				42
$[Fe^{IV}(O)(TQA)(MeCN)]^{2+}$ (**14**)	2	650, 900	0.24	−1.05	17(1)	10
$[Fe^{IV}(O)(Me_3NTB)(MeCN)]^{2+}$ (**15**)	1	770	0.02	1.53	28(7)	46
$Fe^{IV}O$ enzyme intermediates						
taurine dioxygenase (TauD-***J***)	2		0.30	−0.88	10.5	3
prolyl 4-hydroxylase	2		0.30	−0.82	15.5	64
halogenase CytC3	2		0.30, 0.22	−1.09, −0.70	8.1	52
halogenase SyrB2	2		0.30, 0.23	1.09, 0.76		18
tyrosine hydroxylase	2		0.25	1.27	12.5	65

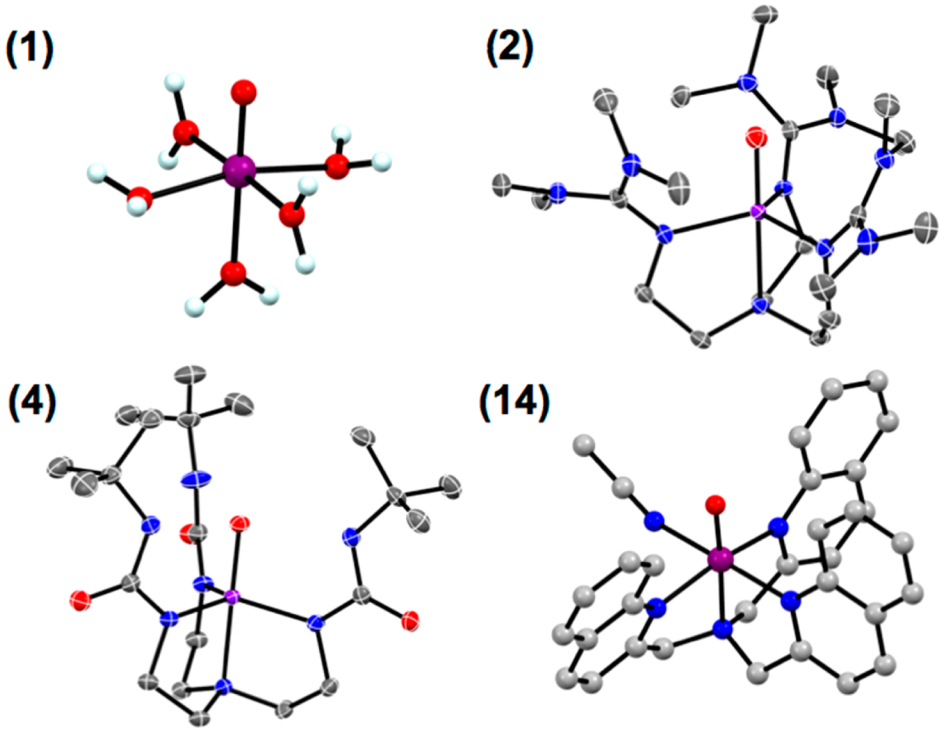

Figure 1. Structures of S = 2 oxoiron(IV) complexes **1** and **14**, based on DFT-derived coordinates from refs 8 and 10, and of **2** and **4**, based on crystallographic data from refs 11 and 12.

supported by weak-field aqua ligands. Complex **1** was found to be a powerful oxidant that can undergo fast hydrogen-atom transfer (HAT) reactions with a range of organic substrates.[9] While the isomer shift of 0.38(2) mm s^{-1} found for **1** made it a

DOI: 10.1021/acs.accounts.5b00244
Acc. Chem. Res. 2015, 48, 2443−2452

close spectroscopic analogue to TauD-*J*, its short half-life of 7 s at 25 °C and the aqueous medium have limited further studies. Since then, our group and others have attempted to address the discrepancy in electronic structure between enzymatic and synthetic oxoiron(IV) systems by synthesizing S = 2 oxoiron(IV) complexes supported by polydentate ligands. This Account focuses on synthetic strategies that may be employed to stabilize the S = 2 ground state, as illustrated by the high-spin oxoiron(IV) complexes in Figure 1.

From the d-orbital splitting diagram for a pseudo-octahedral metal−oxo center, first detailed by Ballhausen and Gray in 1962 and revisited recently by Winkler and Gray,[13] it can be seen that the energy gap between the $d_{x^2-y^2}$ and d_{xy} orbitals competes with the spin-pairing energy to determine whether an S = 1 intermediate-spin state or an S = 2 high-spin state is formed (Figure 2, left). Therefore, the key to achieving an S = 2 spin

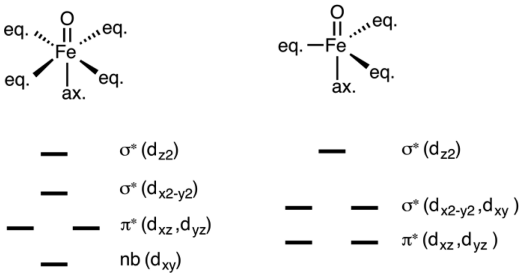

Figure 2. Splitting patterns for d orbitals associated with oxoiron(IV) complexes in (left) pseudo-octahedral and (right) trigonal-bipyramidal geometries.

state is to diminish the energy gap between the d_{xy} and $d_{x^2-y^2}$ orbitals. There are a number of synthetic approaches to achieve this goal. In section 2 we describe the use of bulky tripodal ligands to enforce a trigonal-bipyramidal geometry about the oxoiron(IV) center, thereby making the d_{xy} and $d_{x^2-y^2}$ orbitals degenerate (Figure 2, right) and allowing for an S = 2 ground state. In sections 3 and 4, we highlight different attempts to decrease the energy gap between the d_{xy} and the $d_{x^2-y^2}$ orbital in a pseudo-octahedral geometry, leading in some instances to stabilization of the S = 2 ground state.

2. TRIGONAL-BIPYRAMIDAL S = 2 OXOIRON(IV) COMPLEXES

The majority of reported synthetic oxoiron(IV) complexes have an S = 1 ground state, likely because of a combination of the relatively strong-field ligands employed, namely, tertiary amines and pyridines, and the six-coordinate pseudo-octahedral geometry these complexes adopt, leading to pairing of electrons in the lowest-lying d_{xy} orbital (Figure 2, left). In contrast, the geometry of enzymatic S = 2 oxoiron(IV) species is still under debate, with both trigonal-bipyramidal and pseudo-octahedral configurations being plausible. Theoretical calculations performed on TauD-*J* by Neese supported the possibility of either geometry,[4] while the recent analysis of nuclear resonance vibrational spectroscopy data by Solomon favored a trigonal-bipyramidal geometry for the oxoiron(IV) intermediate in the halogenase SyrB2.[14]

With this in mind, one synthetic strategy to diminish the energy gap between the d_{xy} and $d_{x^2-y^2}$ orbitals is to move away from the six-coordinate pseudo-octahedral geometry adopted by the majority of oxoiron(IV) complexes and toward a C_3-symmetric trigonal-bipyramidal geometry, where the d_{xy} and $d_{x^2-y^2}$ orbitals become degenerate, guaranteeing population of four unpaired electrons and access to an S = 2 ground state (Figure 2, right).

The first example of a trigonal-bipyramidal S = 2 oxoiron(IV) complex came from our group in 2009 when postdoctoral associate Jason England utilized the sterically bulky TMG_3tren ligand to stabilize the oxoiron(IV) species $[Fe^{IV}(O)(TMG_3tren)]^{2+}$ (**2**) (Figures 1 and 3).[15] The benefits of the

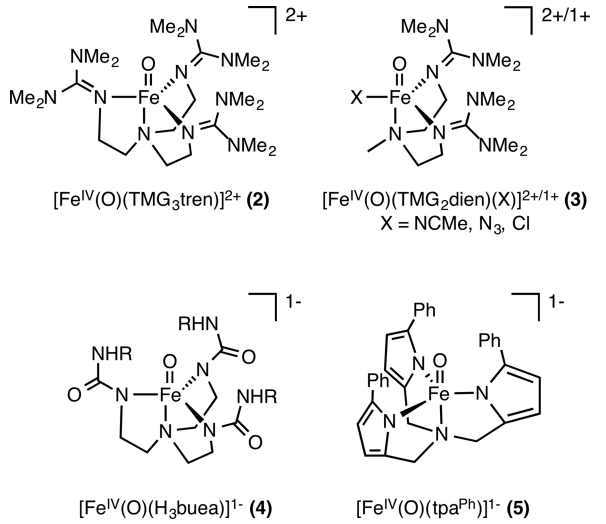

Figure 3. Synthetic trigonal-bipyramidal S = 2 oxoiron(IV) complexes.

tripodal tetradentate ligand were twofold: first, the electron-richness of the imine donors helped stabilize the high-valent Fe^{IV} oxidation state; second, the steric bulk of the six dimethylamine end caps enforced the C_3 symmetry while preventing formation of undesired (μ-oxo)diferric byproducts. Mössbauer spectroscopy of **2** revealed a quadrupole doublet with δ = 0.09 mm s^{-1} and ΔE_Q = −0.29 mm s^{-1}. While the isomer shift of **2** was notably smaller than that of the enzymatic intermediate TauD-*J*, high-field Mössbauer experiments established **2** to have an S = 2 ground state (Table 1).

Compared to its S = 1 counterparts characterized at that time, species **2** was relatively unstable, with a $t_{1/2}$ of 30 s at 25 °C. Closer inspection of the self-decay of **2** revealed an intramolecular pathway through which the reactive S = 2 oxoiron(IV) center attacked one of the terminal methyl groups of the ligand to form an alkoxoiron(III) product.[11] This result demonstrated that the Fe^{IV}=O unit of **2** was reactive enough to cleave a C−H bond with a bond strength of ∼93 kcal mol^{-1} within a few minutes at 25 °C. Indeed, upon perdeuteration of the methyl groups in TMG_3tren to form d_{36}-TMG_3tren, a large KIE of 24 was observed at 25 °C, and the increased stability of the $[Fe^{IV}(O)(d_{36}\text{-}TMG_3tren)]^{2+}$ isotopomer allowed its isolation and crystallization to afford the first structure of a synthetic high-spin oxoiron(IV) species (Figure 1).[11] Complex **2** was found to have an Fe^{IV}=O distance of 1.661(2) Å and an Fe^{IV}=O stretch of 843 cm^{-1}. These values were comparable to those reported for structurally characterized S = 1 oxoiron(IV) species,[5] consistent with the expectation that the Fe^{IV}=O bond order should be independent of the spin state.

The same steric constraints of the TMG_3tren ligand that enforce the C_3 symmetry are also responsible for the diminished reactivity between **2** and external organic substrates. Steric hindrance by the ligand is best illustrated by the

DOI: 10.1021/acs.accounts.5b00244
Acc. Chem. Res. 2015, 48, 2443−2452

difference in the rates of oxidation of 1,4-cyclohexadiene (CHD) and 9,10-dihydroanthracene (DHA). While these substrates have approximately the same C−H bond dissociation energy (BDE), the oxidation of DHA was 13 times slower than that of CHD,[15] consistent with greater steric hindrance from the approach of the bulkier DHA to the oxo moiety. In contrast, CHD and DHA were oxidized at comparable rates by other oxoiron(IV) species such as $[Fe^{IV}(O)(TMC)(MeCN)]^{2+}$.[16]

In order to provide greater access to the Fe^{IV}=O unit, England subsequently converted the tetradentate ligand TMG_3tren to the facial tridentate ligand TMG_2dien, in which one of the TMG_3tren donor arms was replaced with a methyl group.[17] The corresponding oxoiron(IV) species $[Fe^{IV}(O)TMG_2dien(MeCN)]^{2+}$ (**3-MeCN**) (Figure 3) retained the S = 2 ground state of **2**, with similar Mössbauer parameters of δ = 0.08 mm s^{-1} and ΔE_Q = 0.58 mm s^{-1} (Table 1). However, the reactivity of **3-MeCN** was found to greatly surpass that of **2**, with a 630-fold increase in the DHA oxidation rate. In addition, the MeCN ligand in **3-MeCN** could be replaced by Cl^- and N_3^- to form **3-Cl** and **3-N_3**, respectively. Notably, **3-Cl** exhibited an Fe^{IV}−Cl bond distance of 2.27 Å as measured by EXAFS, comparable to the Fe^{IV}−Cl distance of 2.31 Å found for the SyrB2 intermediate.[18]

Using a parallel strategy, Borovik and co-workers reported the structural characterization of a different trigonal-bipyramidal S = 2 oxoiron(IV) species, $[Fe^{IV}(O)(H_3buea)]^{1-}$ (**4**) (Figures 1 and 3).[12] Like TMG_3tren, H_3buea is a tripodal N_4 ligand with bulky end caps, but the equatorial donors are anionic. The negatively charged ligand gave rise to an oxoiron(IV) complex with Mössbauer parameters of δ = 0.02 mm s^{-1} and ΔE_Q = 0.43 mm s^{-1} (Table 1). Complex **4** has an Fe^{IV}=O bond length of 1.680(1) Å, slightly longer than that reported for **2** (1.661(2) Å) (Figure 1), and an Fe^{IV}=O stretch of 799 cm^{-1} in its IR spectrum, 44 cm^{-1} weaker than that found for the shorter Fe^{IV}=O bond of **2**.[12] Perhaps the most interesting feature of the chemistry of **4** is the fact that it was generated by one-electron oxidation of its iron(III) congener $[Fe^{III}(O)(H_3buea)]^{2-}$ (**4_{red}**), which has also been structurally characterized.[19] The H_3buea ligand was designed to provide a hydrogen-bond donor on each arm of the tripod to interact with the oxo ligand. These interactions were clearly observed for the oxo ligand of **4_{red}** but significantly diminished for the oxo ligand in **4**, reflecting the change in the nucleophilicity of the oxo ligand upon oxidation of the iron(III) center to iron(IV) as well as the shift of the iron(IV) center away from the plane of the urea H-bond donors in complex **4**.[12]

Similarly, Chang and co-workers utilized a tripodal tris(pyrrolide) ligand scaffold to support another trigonal-bipyramidal S = 2 oxoiron(IV) center, $[Fe^{IV}(O)(tpa^{Ph})]^-$ (**5**) (Figure 3),[20] which, like **2**, has a Mössbauer isomer shift of 0.09 mm/s (Table 1). Its reactivity with organic substrates reflected a sterically protected oxoiron(IV) center. Although **5** did not react with triphenylphosphine, it did oxidize the less bulky and more easily oxidized dimethylphenylphosphine to the corresponding phosphine oxide. Similarly, the oxoiron(IV) species was capable of oxidizing CHD but not the more bulky DHA.[20]

3. DINUCLEAR COMPLEXES WITH S = 2 OXOIRON(IV) COMPONENTS

While the trigonal-bipyramidal oxoiron(IV) complexes **2**−**5** did indeed achieve an S = 2 ground state, their Mössbauer isomer shifts (~0.1 mm s^{-1}) were notably smaller than those of TauD-*J* and related enzyme intermediates (~0.3 mm s^{-1}). Moreover, their intermolecular reactivity was limited by the steric constraints on access to the oxo moiety imposed by the ligand. For this reason, our group sought out alternate strategies to obtain S = 2 oxoiron(IV) complexes.

In the course of developing models for high-valent diiron intermediates of methane monooxygenase and class 1A ribonucleotide reductases,[21−23] postdoctoral associate Genqiang Xue discovered an interesting series of diiron complexes supported by the tetradentate ligand TPA* (Figure 4). TPA* is

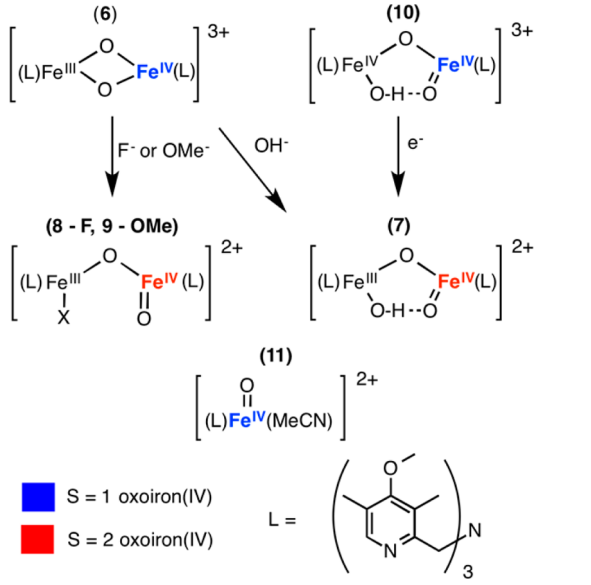

Figure 4. Generation of terminal S = 2 oxoiron(IV) centers in a diiron framework, where each iron center is supported by the electron-rich TPA ligand TPA*.

an electron-rich derivative of tris(2-pyridylmethyl)amine (TPA) with electron-donating substituents at the 3-, 4-, and 5-positions of all three pyridines to stabilize a highly reactive terminal oxoiron(IV) center. In this series of (L)Fe−O−Fe^{IV}(O)(L) complexes, the left-hand (L)Fe−O fragment can be construed as the sixth ligand of the right-hand Fe^{IV}(O)(L) unit. We found that the oxidation state of the left-hand fragment could be used to tune the spin state of the adjacent terminal oxoiron(IV) center, leading to the most reactive oxoiron(IV) complexes to date.

Starting with the $S = {}^3/_2$ diamond-core complex $[Fe^{III}Fe^{IV}(\mu\text{-}O)_2(TPA^*)_2]^{3+}$ (**6**) (Figure 4), Xue found that adding hydroxide, fluoride, or methoxide opened up the diamond core to generate $S = {}^1/_2$ derivatives with antiferromagnetically coupled ($S_a = {}^5/_2$ Fe^{III}−X)/(S_b = 2 Fe^{IV}=O) species featuring a high-spin terminal oxoiron(IV) center (**7**, **8**, and **9**, respectively).[24−28] In the course of this investigation, we also obtained **10**, the one-electron-oxidized derivative of **7**, which was characterized to have a ferromagnetically coupled (S_a = 1 Fe^{IV}−OH)/(S_b = 1 Fe^{IV}=O) center (Figure 4 and Table 1). We speculate that the spin states of the terminal oxoiron(IV) units in **7** and **10** differ because of the nature of the adjacent (HO)(TPA*)Fe−O^- unit. The more reduced HO−Fe^{III}−O^- unit of **7** should be a better π donor than the corresponding HO−Fe^{IV}−O^- unit in **10**, leading to a decrease in the ligand-field splitting of the Fe^{IV}=O unit in **7** that gives rise to its observed S = 2 spin state. Complexes **7**−**10** thus constitute a unique set of structurally related complexes supported by the

DOI: 10.1021/acs.accounts.5b00244
Acc. Chem. Res. 2015, 48, 2443−2452

same tetradentate ligand but having a terminal oxoiron(IV) center in either an $S = 1$ or 2 spin state, which affects their HAT abilities.

Because of the thermal instability of **7**–**9**, their HAT reactivities had to be probed at −80 °C with DHA as the substrate (Figure 5). Notably, the three diiron complexes

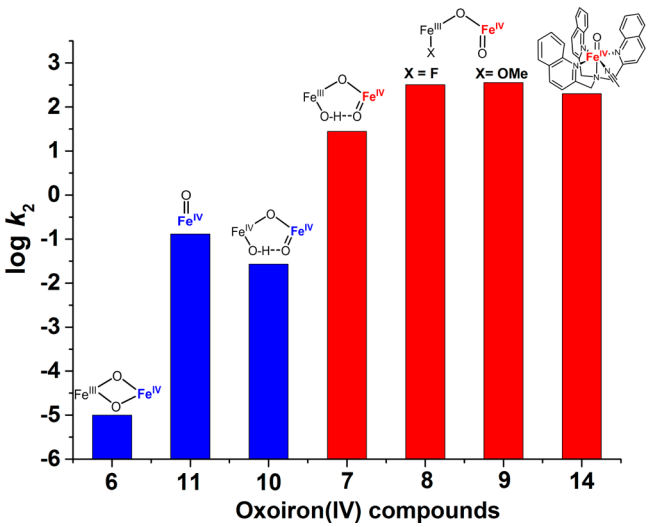

Figure 5. Second-order rate constants for the reaction of oxoiron(IV) complexes with 9,10-dihydroanthracene (DHA) at −80 °C. Red and blue bars indicate complexes with $S = 2$ and $S = 1$ oxoiron(IV) centers, respectively. All of the iron centers are supported by the TPA* ligand except that in **14**, which is supported by the TQA ligand.

containing a terminal $S = 2$ oxoiron(IV) unit, **7**–**9**, demonstrated the highest rates of DHA oxidation.[24] The 10-fold higher reactivity of **8** and **9** is attributed to the absence of the hydrogen bond between the Fe^{III}–OH and Fe^{IV}=O units in **7**.[27] Complex **7** in turn reacts 3000-fold faster than **10**, which has a terminal $S = 1$ oxoiron(IV) unit. Notably, these two complexes constitute the only pair of complexes in which the oxoiron(IV) units are in nearly identical environments but have different spin states and provide the strongest experimental argument thus far in favor of the higher reactivity of the $S = 2$ oxoiron(IV) unit, as predicted by computational methods.[29−33] Complex **10** in turn was 1000-fold more reactive than the diamond-core complex **6**, demonstrating that a terminal oxo unit is better at HAT than a bridging oxo unit. Overall, the series of five diiron complexes **6**–**10** shown in Figure 5 represent an impressive 34-million-fold range in HAT reactivity.[24]

4. OXOIRON(IV) COMPLEXES SUPPORTED BY STERICALLY HINDERED TPA LIGANDS

Despite our success in generating $S = 2$ oxoiron(IV) species supported by electron-rich TPA ligands, these reactive centers were housed within a diiron core, making them less faithful analogues of mononuclear non-heme iron enzyme active sites. Furthermore, the thermal instability of the most reactive complexes required reactivity studies to be carried out only at −80 °C, a temperature too low for substrates with strong C–H bonds to be oxidized. We thus focused on generating an $S = 2$ oxoiron(IV) complex within a mononuclear six-coordinate environment.

One strategy to diminish the energy gap between the d_{xy} and $d_{x^2-y^2}$ orbitals within a six-coordinate oxoiron(IV) environment is to weaken the equatorial ligand field and decrease the $d_{x^2-y^2}$ orbital energy. For example, by replacing the relatively strong-field pyridine ligands that support many of synthetic oxoiron(IV) complexes with weaker-field donors, one could in principle attain an $S = 2$ ground state. Indeed, the successful generation of the aqueous oxoiron(IV) complex **1**[8] serves to demonstrate the viability of this approach, but analogous attempts to employ carboxylate ligands have not yet led to $S = 2$ oxoiron(IV) complexes sufficiently stable to characterize.[34−36]

We thus applied a modified strategy by modulating the steric environment around the TPA pyridine nitrogen atoms to weaken the ligand field about the iron center. Such an approach was used in the 1990s to tune the spin states of various Fe(TPA) complexes, where the introduction of one or more α-substituents on the pyridine rings of TPA generated a steric interaction between the Fe center and the H atoms of the α-substituent, preventing the formation of the short $Fe-N_{Py}$ bonds necessary to adopt lower-spin configurations.[37] The steric effect of α-methyl substitution on the pyridine rings is clearly illustrated in the ^{1}H NMR spectra of two $[Fe^{II}(L)(MeCN)_2](ClO_4)$ complexes. The spectrum of the L = TPA complex is consistent with a diamagnetic low-spin $S = 0$ species (Figure 6, top), while that of the L = $6Me_3$TPA complex

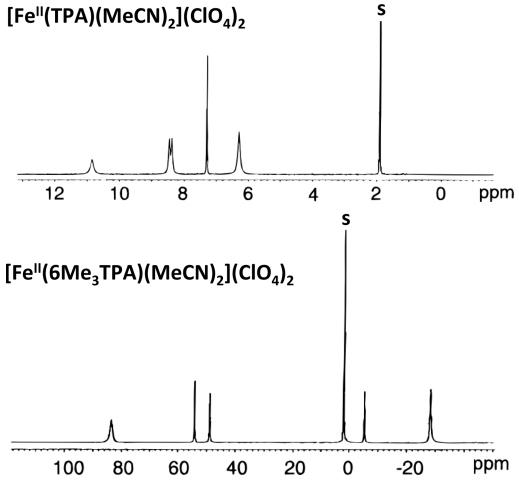

Figure 6. ^{1}H NMR spectra of (top) $S = 0$ $[Fe^{II}(TPA)(MeCN)_2](ClO_4)_2$ and (bottom) $S = 2$ $[Fe^{II}(6Me_3TPA)(MeCN)_2](ClO_4)_2$ in CD_3CN. Reproduced from ref 37. Copyright 1997 American Chemical Society.

instead reveals a paramagnetic high-spin $S = 2$ species (Figure 6, bottom). In fact, it was found that only a single methyl α-substituent was sufficient to trigger a spin-state change in this $(TPA)Fe^{II}$ family of compounds (Table 2).[37]

The same strategies to enforce spin-state changes within stable Fe^{II} coordination complexes extended to reactive Fe^{III}–peroxo intermediates as well. The alkylperoxoiron(III) intermediates $[Fe^{III}(TPA)(OH_2)(OO^tBu)]^+$ and $[Fe^{III}(6Me_3TPA)(OH_2)(OO^tBu)]^+$ were distinguished in having an $S = {}^1/_2$ Fe^{III} center for the former and an $S = {}^5/_2$ Fe^{III} center for the latter. Interestingly, the complex with one α-substituent, $[Fe^{III}(6MeTPA)(OH_2)(OO^tBu)]^+$, consisted of a mixture of low-spin Fe^{III} and high-spin Fe^{III} centers, hinting at the flexibility of this synthetic strategy to provide access to intermediate points prior to a complete spin-state change (Table 2).[37]

DOI: 10.1021/acs.accounts.5b00244
Acc. Chem. Res. 2015, 48, 2443−2452

Table 2. Spin States of Complexes Supported by TPA Ligands versus the Number of α-Substituents (N_{sub}) on the Pyridine Rings

	$N\alpha\text{-}_{sub}$ = 0	$N\alpha\text{-}_{sub}$ = 1	$N\alpha\text{-}_{sub}$ = 3	ref(s)
$(L)Fe^{II}(MeCN)_2$	0	0	2	37
$(L)Fe^{III}(OOR)$	$^1/_2$	$^1/_2$ and $^5/_2$	$^5/_2$	37
$(L)Fe^{III}(O)_2Fe^{IV}(L)$	$^3/_2$ [$^1/_2$, 1]	$^1/_2$ [$^5/_2$, 2]	$^1/_2$ [$^5/_2$, 2]	38−41
$(L)Fe^{IV}(O)(MeCN)$	1	1	2	10, 42, 57

Gratifyingly, this same synthetic strategy could be extended to oxodiiron(III/IV) systems. In 1995, an $[Fe^{III}Fe^{IV}(\mu\text{-}O)_2(TPA)_2]^{3+}$ diamond-core complex was identified and described as having valence-delocalized (S_a = $^1/_2$ Fe^{III})/(S_b = 1 Fe^{IV}) centers with a system spin of S = $^3/_2$.[38,39] The corresponding complexes with 6MeTPA or $6Me_3$TPA instead gave rise to valence-localized (S_a = $^5/_2$ Fe^{III})/(S_b = 2 Fe^{IV}) centers with a system spin of S = $^1/_2$ as a result of antiferromagnetic coupling of the two iron components.[40,41] Thus, the introduction of even one α-substituent was sufficient to trigger a change in the spin states of both Fe centers from low-spin to high-spin (Table 2). Further characterization of $[Fe^{III}Fe^{IV}(O)_2(6Me_3TPA)_2]^{3+}$ by resonance Raman spectroscopy revealed an Fe^{IV}═O vibration at 840 cm^{-1},[41] a frequency similar to those associated with $[Fe^{IV}(O)(TMC)(MeCN)]^{2+}$ (S = 1) and **2** (S = 2), suggesting that the S = 2 Fe^{IV} unit was in fact a terminal oxoiron(IV) center.[15,35] The diiron(III/IV) complexes of 6MeTPA and $6Me_3$TPA showed for the first time that synthetic S = 2 oxoiron(IV) centers could be obtained, albeit within a diiron framework. While the reactivity of these complexes has not been investigated, they are closely related to the S = $^1/_2$ diiron complexes supported by the electron-rich TPA* ligand discussed in the preceding section, **7**−**9**, for which very high rates of oxidation of DHA have been reported (Figure 5).

With evidence that this synthetic strategy could stabilize a terminal S = 2 oxoiron(IV) center in a diiron framework, our group attempted to apply these ideas to the generation of mononuclear S = 2 oxoiron(IV) species by modifying the parent S = 1 $[Fe^{IV}(O)(TPA)(MeCN)]^{2+}$ complex (Figure 7). In 2006, we reported the characterization of oxoiron(IV) complexes of 6MeTPA and QBPA (**12** and **13**, respectively; Figure 7) that were obtained by reactions of peracetic acid with their iron(II) precursors.[42] The new species **12** and **13** exhibited respective near-IR absorption features of λ_{max} = 770 and 775 nm, which were red-shifted compared with that of $[Fe^{IV}(O)(TPA)(MeCN)]^{2+}$ (λ_{max} = 720 nm), indicating a weakening of the ligand field ($\Delta\nu \sim 900$ cm^{-1}) (Table 1). Importantly, these results indicated that the steric effect of a hydrogen atom on an sp^3-hybridized α-carbon substituent (6MeTPA) was comparable to that on an sp^2-hybridized α-carbon substituent (QBPA).[42] However, in neither case did the ground spin state of the oxoiron(IV) center deviate from S = 1. Although DFT calculations by Ghosh predicted that a TPA ligand with three α-substituents (Figure 8) should lead to an S = 2 oxoiron(IV) center,[43] attempts at that time to obtain oxoiron(IV) complexes of such ligands were not successful, suggesting that the right reaction conditions had not yet been found to stabilize species that are likely to be more reactive than the S = 1 complexes **12** and **13**.

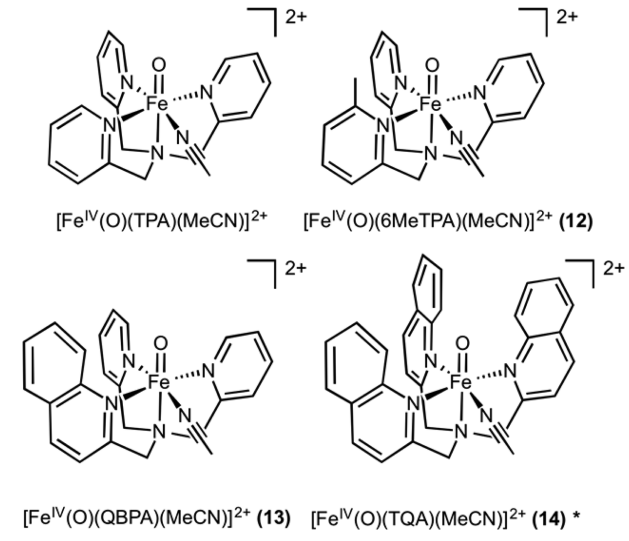

Figure 7. Synthetic oxoiron(IV) complexes supported by TPA and derivatives. The asterisk indicates a complex with an S = 2 ground state.

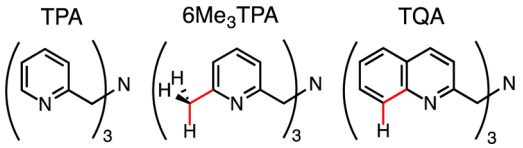

Figure 8. TPA ligand and derivatives with α-substituents.

Three years later, we discovered the utility of 2-(*tert*-butylsulfonyl)iodosylbenzene (ArIO)[44] as an oxidant to synthesize the S = 2 oxoiron(IV) complex **2**.[15] We ascribe our success in synthesizing **2** by this method to the efficiency of O-atom transfer from ArIO to the iron(II) precursor and the steric barriers that minimized comproportionation of the $Fe^{IV}(O)$ product with residual precursor. This strategy was subsequently applied by postdoctoral associate Achintesh Biswas for the successful generation of the oxoiron(IV) complex supported by the TQA ligand (Figure 8).[10]

We reported the synthesis of $[Fe^{IV}(O)(TQA)(MeCN)]^{2+}$ (**14**) (Figure 7) at −40 °C earlier this year[10] and found it to have a $t_{1/2}$ of only 15 min at −40 °C. Mössbauer studies established it as an S = 2 oxoiron(IV) complex with an isomer shift of 0.24 mm s^{-1}, which makes it the only synthetic high-spin oxoiron(IV) complex to have an isomer shift that falls within the range of values found for enzymatic oxoiron(IV) intermediates (0.22−0.30 mm s^{-1}; Table 1). Furthermore, among synthetic oxoiron(IV) complexes characterized to date, the magnetic hyperfine parameters deduced for **14** from the analysis of high-field Mössbauer data[10] most closely resemble those found for TauD-J[3] and the corresponding intermediate for prolyl-4-hydroxylase,[64] making **14** the closest electronic model for these high-spin oxoiron(IV) enzyme intermediates to date.

This resemblance leads us to ask why **14**, of all the synthetic oxoiron(IV) complexes characterized, should have an isomer shift most similar to those of the enzyme intermediates, given

DOI: 10.1021/acs.accounts.5b00244
Acc. Chem. Res. 2015, 48, 2443−2452

that its donor set does not match the 2-His-2-carboxylate combination associated with TauD-*J*. All other $S = 2$ oxoiron(IV) complexes with N-donor sets listed in Table 1 have isomer shifts of 0.12 mm s^{-1} or smaller, while that of $[Fe^{IV}(O)(OH_2)_5]^{2+}$ (**1**)[8,10] at 0.38 mm s^{-1} is above the range for enzyme intermediates. As the isomer shift reflects the donation of electron density from the ligands into the iron 4s orbital, TQA must represent a good electronic approximation of the donor set found in the enzyme active sites. Indeed, DFT calculations predict **14** to have the experimentally observed isomer shift of 0.24 mm s^{-1}.[10] Additional examples of $S = 2$ oxoiron(IV) complexes with isomer shifts falling into this range would obviously help to clarify the factors that govern the isomer shifts, and hence the electronic environments, of oxoiron(IV) enzyme intermediates.

Complex **14** also appears to be a good functional model for TauD-*J*. Its thermal instability translates into high intermolecular HAT reactivity. Complex **14** exhibits the highest rates of substrate oxidation by a synthetic oxoiron(IV) complex in an organic solvent and cleaves the strong C−H bonds of cyclohexane (BDE ≈ 99 kcal/mol) with a rate constant (k_2) of 0.37 M^{-1} s^{-1} at −40 °C. For comparison, its $S = 1$ analogue $[Fe^{IV}(O)(TPA)(MeCN)]^{2+}$ is not able to oxidize cyclohexane at all at −40 °C, suggesting that the simple substitution of pyridine rings with quinoline rings not only changes the spin state but also dramatically enhances the reactivity profile.[10] In fact, after temperature adjustment, the rate of cyclohexane oxidation by **14** approaches that for the oxidation of taurine by TauD-*J* at 5 °C.[45]

To be able to place the HAT reactivity of **14** and those of the dinuclear $S = 2$ oxoiron(IV) complexes **7**−**9** within a common framework, we measured the DHA oxidation rate of **14** at −80 °C and obtained a k_2 value of 200 M^{-1} s^{-1} (Figure 9). This

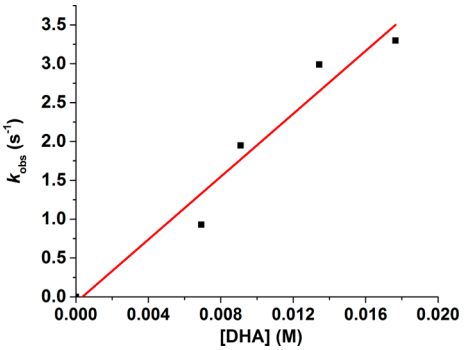

Figure 9. Plot of the pseudo-first-order rate constant k_{obs} vs DHA concentration for the reaction of **14** (1.0 mM) with DHA in a 3:1 acetone-d_6/acetonitrile-d_3 mixture at −80 °C.

comparison shows that **14** is almost as reactive with DHA as **8** and **9** (Figure 5). This is an important point, as it suggests that the high reactivity of these species is independent of whether the $S = 2$ $Fe^{IV}(O)$ unit is in a mononuclear or a dinuclear framework. These results further support our idea that the $(X)(TPA^*)Fe^{III}-O^-$ unit in these dinuclear systems can be construed simply as a sixth ligand for the $S = 2$ oxoiron(IV) center.

Figure 5 allows us to establish a relationship between spin state and HAT reactivity for oxoiron(IV) centers supported by TPA-based ligands, where $S = 2$ oxoiron(IV) centers appear to be more reactive than $S = 1$ oxoiron(IV) centers. However, replacing the three quinoline donors of TQA with *N*-methylbenzimidazole donors in Me_3NTB gives the $S = 1$ complex $[Fe^{IV}(O)(Me_3NTB)(MeCN)]^{2+}$ (**15**) (Table 1), which exhibits HAT reactivity comparable to that of **14** despite having a different ground spin state.[10,46] This apparent paradox is illustrated by the plot of log k_2' versus C−H bond dissociation energy in Figure 10, where the HAT oxidation rates measured

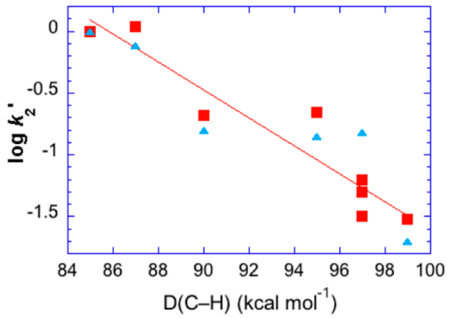

Figure 10. Plot of log k_2' vs C−H bond dissociation energy for the reactions of hydrocarbons with **14** (red) and **15** (blue) at −40 °C in CH_3CN. The k_2' values are second-order rate constants normalized by the number of equivalent substrate C−H bonds that can be attacked. Reproduced from ref 10. Copyright 2015 American Chemical Society.

for the two complexes fall on the same line. Thus, an $S = 1$ oxoiron(IV) complex can be just as reactive as an $S = 2$ oxoiron(IV) complex. It is hypothesized that the high reactivity of **15** may arise from a low-lying $S = 2$ excited state, but additional experimental data would be helpful to shed further light on this puzzling comparison.

5. CHALLENGES

Through the use of different synthetic strategies, we and others have generated $S = 2$ oxoiron(IV) complexes in both trigonal-bipyramidal and pseudo-octahedral geometries to shed light on why such centers are used to effect HAT in enzymes like TauD. In this Account, we have focused on the role of the spin state and provided experimental evidence that the $S = 2$ ground state can lead to enhanced HAT reactivity relative to $S = 1$ oxoiron(IV) complexes supported by similar ligand scaffolds (Figure 5). However, as exemplified by the reactivity of the $S = 1$ complex **15** (Figure 10), this correlation does not strictly hold, and further investigation of the factors that control the reactivity is required. In particular, Mayer has argued that the HAT reactivity of an oxoiron(IV) complex is related to the strength of the O−H bond formed in the reaction, which in turn depends on the $Fe^{IV/III}$ potential and the pK_a of the Fe^{III}−OH moiety,[47] but these properties have proven difficult to measure. Indeed, only Borovik has thus far been able to determine such thermodynamic properties for an oxoiron(IV) complex.[48]

Among other challenges are the trapping and characterization of the proposed $S = 2$ oxoiron(IV) intermediate generated upon reaction of O_2 with $[Fe^{II}(Tp^{Ph2})(Y)]$ (Tp^{Ph2} = hydridotris(3,5-diphenylpyrazolyl)borate; Y = $PhC(O)CO_2^-$ or $Ph_2C(OH)CO_2^-$), which respectively are functional models for non-heme iron enzymes that use 2-oxo- or 2-hydroxoacids as electron sources for O_2 activation.[49,50] This putative oxidant is responsible for the observed hydroxylation of a phenyl ring of the Tp^{Ph2} supporting ligand. Moreover, it can also effect intermolecular oxidation of cyclohexane and *n*-butane in competition with the intramolecular ligand hydroxylation.[16]

DOI: 10.1021/acs.accounts.5b00244
Acc. Chem. Res. 2015, 48, 2443−2452

A different synthetic challenge is to mimic the reactivity of the non-heme iron halogenases CytC3 and SyrB2, which convert substrate C−H bonds into C−X (X = Cl, Br) bonds via an S = 2 $Fe^{IV}(O)(X)$ intermediate.[51,52] Modeling of these enzymes requires the generation of S = 2 oxoiron(IV) complexes with halide ligands coordinated *cis* to the oxo moiety and the demonstration of halide transfer to a C−H bond. This is a research direction that is clearly of interest to us[17] and to the groups of Comba[53] and Costas.[54]

Finally, S = 2 oxoiron(IV) complexes with oxygen-rich ligand environments related to $[Fe^{IV}(O)(OH_2)_5]^{2+}$ (**1**) would be welcome additions to this family. There are two intriguing recent developments relevant to this Account. Nocera and coworkers employed sterically bulky alkoxide ligands to make a trigonal $Fe^{II}(OR)_3^-$ complex. When reacted with PhIO or Me_3NO, this complex forms a highly reactive species that is proposed by DFT to have a pseudotetrahedral S = 2 oxoiron(IV) center.[55] In a different approach, Long and coworkers exploited the weak-field carboxylate donors that support iron(II) centers in a metal−organic framework to generate a reactive iron-based intermediate upon reaction with N_2O that is capable of oxidizing ethane to ethanol.[56] While no direct spectroscopic information is currently available, computational studies suggest that this intermediate is a pseudo-octahedral S = 2 oxoiron(IV) species.[57,58] Clearly, these creative synthetic strategies will unveil even more interesting chemistry related to S = 2 oxoiron(IV) complexes in the future.

AUTHOR INFORMATION

Corresponding Author

*E-mail: larryque@umn.edu.

Notes

The authors declare no competing financial interest.

Biographies

Mayank Puri grew up in Philadelphia, where he was first introduced to the joys of chemistry and Wawa. He obtained his bachelor's degree from Brandeis University, during which time he carried out undergraduate research in the organometallic chemistry lab of Professor Oleg V. Ozerov. Upon graduating in 2008, he worked at a startup chemical company, QD Vision, where he synthesized semiconductor nanocrystals (quantum dots) for display applications. He then started his Ph.D. studies at the University of Minnesota in 2010 and joined the Que group to explore the chemistry of high-spin oxoiron(IV) complexes.

Lawrence Que, Jr., discovered chemistry as a young boy growing up in Manila because of his interest in performing magic tricks. He obtained his Ph.D. in chemistry from the University of Minnesota in 1973 and did postdoctoral stints with Richard Holm and Eckard Münck. He is currently Regents Professor at the University of Minnesota. His long-term research interests have focused on how biological non-heme iron centers activate dioxygen to carry out an amazing array of oxidative transformations. These efforts led to the first crystal structure of a synthetic non-heme oxoiron(IV) complex in 2003, introducing a new class of iron complexes for detailed investigation. His achievements in high-valent non-heme iron chemistry have been recognized by several awards, including the ACS Alfred Bader Award in Bioorganic or Bioinorganic Chemistry (2008) and the RSC Inorganic Reaction Mechanisms Award (2011).

ACKNOWLEDGMENTS

Recent work in the Que laboratory has been supported by National Science Foundation Grant CHE-1361773 and National Institutes of Health Grant GM38767. M.P. thanks the University of Minnesota Graduate School for a doctoral dissertation fellowship.

REFERENCES

(1) Costas, M.; Mehn, M. P.; Jensen, M. P.; Que, L., Jr. Oxygen Activation at Mononuclear Nonheme Iron: Enzymes, Intermediates, and Models. *Chem. Rev.* **2004**, *104*, 939−986.

(2) Krebs, C.; Fujimori, D. G.; Walsh, C. T.; Bollinger, J. M., Jr. Non-Heme Fe(IV)−Oxo Intermediates. *Acc. Chem. Res.* **2007**, *40*, 484−492.

(3) Price, J. C.; Barr, E. W.; Tirupati, B.; Bollinger, J. M., Jr.; Krebs, C. The First Direct Characterization of a High-Valent Iron Intermediate in the Reaction of an a-Ketoglutarate-Dependent Dioxygenase: A High-Spin Fe(IV) Complex in Taurine/a-Ketoglutarate Dioxygenase (TauD) from Escherichia coli. *Biochemistry* **2003**, *42*, 7497−7508.

(4) Sinnecker, S.; Svensen, N.; Barr, E. W.; Ye, S.; Bollinger, J. M., Jr.; Neese, F.; Krebs, C. Spectroscopic and Computational Evaluation of the Structure of the High-Spin Fe(IV)-Oxo Intermediates in Taurine: α-Ketoglutarate Dioxygenase from Escherichia coli and Its His99Ala Ligand Variant. *J. Am. Chem. Soc.* **2007**, *129*, 6168−6179.

(5) McDonald, A. R.; Que, L., Jr. High-Valent Nonheme Iron-Oxo Complexes: Synthesis, Structure, and Spectroscopy. *Coord. Chem. Rev.* **2013**, *257*, 414−428.

(6) Rohde, J.-U.; In, J.-H.; Lim, M. H.; Brennessel, W. W.; Bukowski, M. R.; Stubna, A.; Münck, E.; Nam, W.; Que, L., Jr. Crystallographic and Spectroscopic Evidence for a Nonheme Fe^{IV}═O Complex. *Science* **2003**, *299*, 1037−1039.

(7) Que, L., Jr. The road to non-heme oxoferryls and beyond. *Acc. Chem. Res.* **2007**, *40*, 493−500.

(8) Pestovsky, O.; Stoian, S.; Bominaar, E. L.; Shan, X.; Münck, E.; Que, L., Jr.; Bakac, A. Aqueous Fe^{IV}═O: Spectroscopic Identification and Oxo Group Exchange. *Angew. Chem., Int. Ed.* **2005**, *44*, 6871−6874.

(9) Pestovsky, O.; Bakac, A. Reactivity of Aqueous Fe(IV) in Hydride and Hydrogen Atom Transfer Reactions. *J. Am. Chem. Soc.* **2004**, *126*, 13757−13764.

(10) Biswas, A. N.; Puri, M.; Meier, K. K.; Oloo, W. N.; Rohde, G. T.; Bominaar, E. L.; Münck, E.; Que, L. Modeling TauD-J: A High-Spin Nonheme Oxoiron(IV) Complex with High Reactivity toward C−H Bonds. *J. Am. Chem. Soc.* **2015**, *137*, 2428−2431.

(11) England, J.; Guo, Y.; Farquhar, E. R.; Young, V. G., Jr.; Münck, E.; Que, L., Jr. The Crystal Structure of a High-Spin Oxoiron(IV) Complex and Characterization of Its Self-Decay Pathway. *J. Am. Chem. Soc.* **2010**, *132*, 8635−8644.

(12) Lacy, D. C.; Gupta, R.; Stone, K. L.; Greaves, J.; Ziller, J. W.; Hendrich, M. P.; Borovik, A. S. Formation, Structure, and EPR Detection of a High Spin Fe^{IV}—Oxo Species Derived from Either an Fe^{III}—Oxo or Fe^{III}—OH Complex. *J. Am. Chem. Soc.* **2010**, *132*, 12188−12190.

(13) (a) Ballhausen, C. J.; Gray, H. B. The Electronic Structure of the Vanadyl Ion. *Inorg. Chem.* **1962**, *1*, 111−122. (b) Winkler, J. R.; Gray, H. B. Electronic Structures of Oxo-Metal Ions. *Struct. Bonding* **2012**, *142*, 17−28.

(14) Wong, S. D.; Srnec, M.; Matthews, M. L.; Liu, L. V.; Kwak, Y.; Park, K.; Bell, C. B., III; Alp, E. E.; Zhao, J.; Yoda, Y.; Kitao, S.; Seto, M.; Krebs, C.; Bollinger, J. M., Jr.; Solomon, E. I. Elucidation of the Fe(IV)═O intermediate in the catalytic cycle of the halogenase SyrB2. *Nature* **2013**, *499*, 320−323.

(15) England, J.; Martinho, M.; Farquhar, E. R.; Frisch, J. R.; Bominaar, E. L.; Münck, E.; Que, L., Jr. A Synthetic High-Spin Oxoiron(IV) Complex: Generation, Spectroscopic Characterization, and Reactivity. *Angew. Chem., Int. Ed.* **2009**, *48*, 3622−3626.

(16) Kleespies, S. T.; Oloo, W. N.; Mukherjee, A.; Que, L. C−H Bond Cleavage by Bioinspired Nonheme Oxoiron(IV) Complexes,

DOI: 10.1021/acs.accounts.5b00244
Acc. Chem. Res. 2015, 48, 2443−2452

Including Hydroxylation of n-Butane. *Inorg. Chem.* **2015**, *54*, 5053−5064.
(17) England, J.; Guo, Y.; Van Heuvelen, K. M.; Cranswick, M. A.; Rohde, G. T.; Bominaar, E. L.; Münck, E.; Que, L., Jr. A More Reactive Trigonal Bipyramidal High-Spin Oxoiron(IV) Complex with a cis-Labile Site. *J. Am. Chem. Soc.* **2011**, *133*, 11880−11883.
(18) Matthews, M. L.; Krest, C. M.; Barr, E. W.; Vaillancourt, F. H.; Walsh, C. T.; Green, M. T.; Krebs, C.; Bollinger, J. M., Jr. Substrate-Triggered Formation and Remarkable Stability of the C−H Bond-Cleaving Chloroferryl Intermediate in the Aliphatic Halogenase, SyrB2. *Biochemistry* **2009**, *48*, 4331−4343.
(19) MacBeth, C. E.; Golombek, A. P.; Young, V. G., Jr.; Yang, C.; Kuczera, K.; Hendrich, M. P.; Borovik, A. S. O_2 Activation by Nonheme Iron Complexes: A Monomeric Fe(III)-Oxo Complex Derived From O_2. *Science* **2000**, *289*, 938−941.
(20) Bigi, J. P.; Harman, W. H.; Lassalle-Kaiser, B.; Robles, D. M.; Stich, T. A.; Yano, J.; Britt, R. D.; Chang, C. J. A High-Spin Iron(IV)−Oxo Complex Supported by a Trigonal Nonheme Pyrrolide Platform. *J. Am. Chem. Soc.* **2012**, *134*, 1536−1542.
(21) Shu, L.; Nesheim, J. C.; Kauffmann, K.; Münck, E.; Lipscomb, J. D.; Que, L., Jr. An $Fe_2^{IV}O_2$ Diamond Core Structure for the Key Intermediate **Q** of Methane Monooxygenase. *Science* **1997**, *275*, 515−518.
(22) Banerjee, R.; Proshlyakov, Y.; Lipscomb, J. D.; Proshlyakov, D. A. Structure of the key species in the enzymatic oxidation of methane to methanol. *Nature* **2015**, *518*, 431−434.
(23) Dassama, L. M.; Silakov, A.; Krest, C. M.; Calixto, J. C.; Krebs, C.; Bollinger, J. M., Jr.; Green, M. T. A 2.8 A Fe-Fe Separation in the Fe Intermediate, X, from Escherichia coli Ribonucleotide Reductase. *J. Am. Chem. Soc.* **2013**, *135*, 16758−16761.
(24) Xue, G.; De Hont, R.; Münck, E.; Que, L., Jr. Million-fold activation of the $[Fe_2(\mu\text{-}O)_2]$ diamond core for C−H bond cleavage. *Nat. Chem.* **2010**, *2*, 400−405.
(25) De Hont, R. F.; Xue, G.; Hendrich, M. P.; Que, L., Jr.; Bominaar, E. L.; Münck, E. Mössbauer, Electron Paramagnetic Resonance, and Density Functional Theory Studies of Synthetic S = 1/2 Fe^{III}−O−Fe^{IV}=O Complexes. Superexchange-Mediated Spin Transition at the Fe^{IV}=O Site. *Inorg. Chem.* **2010**, *49*, 8310−8322.
(26) Xue, G.; Pokutsa, A.; Que, L., Jr. Substrate-Triggered Activation of a Synthetic $[Fe_2(\mu\text{-}O)_2]$ Diamond Core for C−H Bond Cleavage. *J. Am. Chem. Soc.* **2011**, *133*, 16657−16667.
(27) Shanmugam, M.; Xue, G.; Que, L., Jr.; Hoffman, B. M. ^{1}H-ENDOR Evidence for a Hydrogen Bonding Interaction that Modulates the Reactivity of a Non-heme Fe^{IV}=O Unit. *Inorg. Chem.* **2012**, *51*, 10080−10082.
(28) Xue, G.; Geng, C.; Ye, S.; Fiedler, A. T.; Neese, F.; Que, L., Jr. Hydrogen-Bonding Effects on the Reactivity of [X−Fe^{III}−O−Fe^{IV}=O] (X = OH, F) Complexes toward C−H Bond Cleavage. *Inorg. Chem.* **2013**, *52*, 3976−3984.
(29) Decker, A.; Rohde, J.-U.; Klinker, E. J.; Wong, S. D.; Que, L., Jr.; Solomon, E. I. Spectroscopic and Quantum Chemical Studies on Low-Spin Fe^{IV}=O Complexes: Fe-O Bonding and Its Contributions to Reactivity. *J. Am. Chem. Soc.* **2007**, *129*, 15983−15996.
(30) Bernasconi, L.; Louwerse, M. J.; Baerends, E. J. The Role of Equatorial and Axial Ligands in Promoting the Activity of Non-Heme Oxidoiron(IV) Catalysts in Alkane Hydroxylation. *Eur. J. Inorg. Chem.* **2007**, *2007*, 3023−3033.
(31) Geng, C.; Ye, S.; Neese, F. Analysis of Reaction Channels for Alkane Hydroxylation by Nonheme Iron(IV)−Oxo Complexes. *Angew. Chem., Int. Ed.* **2010**, *49*, 5717−5720.
(32) Shaik, S.; Chen, H.; Janardanan, D. Exchange-enhanced reactivity in bond activation by metal−oxo enzymes and synthetic reagents. *Nat. Chem.* **2011**, *3*, 19−27.
(33) Usharani, D.; Janardanan, D.; Li, C.; Shaik, S. A Theory for Bioinorganic Chemical Reactivity of Oxometal Complexes and Analogous Oxidants: The Exchange and Orbital-Selection Rules. *Acc. Chem. Res.* **2013**, *46*, 471−482.
(34) Rohde, J.-U.; Stubna, A.; Bominaar, E. L.; Münck, E.; Nam, W.; Que, L., Jr. Nonheme Oxoiron(IV) Complexes of Tris(2-pyridylmethyl)amine with cis-Monoanionic Ligands. *Inorg. Chem.* **2006**, *45*, 6435−6445.
(35) Jackson, T. A.; Rohde, J.-U.; Seo, M. S.; Sastri, C. V.; DeHont, R.; Stubna, A.; Ohta, T.; Kitagawa, T.; Münck, E.; Nam, W.; Que, L., Jr. Axial Ligand Effects on the Geometric and Electronic Structures of Nonheme Oxoiron(IV) Complexes. *J. Am. Chem. Soc.* **2008**, *130*, 12394−12407.
(36) McDonald, A. R.; Guo, Y.; Vu, V. V.; Bominaar, E. L.; Münck, E.; Que, L., Jr. A Mononuclear Carboxylate-Rich Oxoiron(IV) Complex: a Structural and Functional Mimic of TauD Intermediate. *'J' Chem. Sci.* **2012**, *3*, 1680−1693.
(37) Zang, Y.; Kim, J.; Dong, Y.; Wilkinson, E. C.; Appelman, E. H.; Que, L., Jr. Models for Nonheme Iron Intermediates: Structural Basis for Tuning the Spin States of Fe(TPA) Complexes. *J. Am. Chem. Soc.* **1997**, *119*, 4197−4205.
(38) Dong, Y.; Fujii, H.; Hendrich, M. P.; Leising, R. A.; Pan, G.; Randall, C. R.; Wilkinson, E. C.; Zang, Y.; Que, L., Jr.; Fox, B. G.; Kauffmann, K.; Münck, E. A High-Valent Nonheme Iron Intermediate. Structure and Properties of $[Fe_2(\mu\text{-}O)_2(5\text{-Me-TPA})_2](ClO_4)_3$. *J. Am. Chem. Soc.* **1995**, *117*, 2778−2792.
(39) Hsu, H.-F.; Dong, Y.; Shu, L.; Young, V. G., Jr.; Que, L., Jr. Crystal Structure of a Synthetic High-Valent Complex with an $Fe_2(\mu\text{-}O)_2$ Diamond Core. Implications for the Core Structures of Methane Monooxygenase Intermediate Q and Ribonucleotide Reductase Intermediate X. *J. Am. Chem. Soc.* **1999**, *121*, 5230−5237.
(40) Dong, Y.; Que, L., Jr.; Kauffmann, K.; Münck, E. An Exchange-Coupled Complex with Localized High-Spin Fe^{IV} and Fe^{III} Sites of Relevance to Cluster X of Escherichia coli Ribonucleotide Reductase. *J. Am. Chem. Soc.* **1995**, *117*, 11377−11378.
(41) Zheng, H.; Yoo, S. J.; Münck, E.; Que, L., Jr. The Flexible $Fe_2(\mu\text{-}O)_2$ Diamond Core: A Terminal Iron(IV)-Oxo Species Generated from the Oxidation of a Bis(μ-oxo)diiron(III) Complex. *J. Am. Chem. Soc.* **2000**, *122*, 3789−3790.
(42) Paine, T. K.; Costas, M.; Kaizer, J.; Que, L., Jr. Oxoiron(IV) complexes of the tris(2-pyridylmethyl)amine ligand family: effect of pyridine α-substituents. *J. Biol. Inorg. Chem.* **2006**, *11*, 272−276.
(43) Ghosh, A.; Tangen, E.; Ryeng, H.; Taylor, P. R. Electronic Structure of High-Spin Iron(IV) Complexes. *Eur. J. Inorg. Chem.* **2004**, *2004*, 4555−4560.
(44) Macikenas, D.; Skrzypczak-Jankun, E.; Protasiewicz, J. D. A New Class of Iodonium Ylides Engineered as Soluble Primary Oxo and Nitrene Sources. *J. Am. Chem. Soc.* **1999**, *121*, 7164−7165.
(45) Price, J. C.; Barr, E. W.; Glass, T. E.; Krebs, C.; Bollinger, J. M., Jr. Evidence for Hydrogen Abstraction from C1 of Taurine by the High-Spin Fe(IV) Intermediate Detected during Oxygen Activation by Taurine:a-Ketoglutarate Dioxygenase (TauD). *J. Am. Chem. Soc.* **2003**, *125*, 13008−13009.
(46) Seo, M. S.; Kim, N. H.; Cho, K.-B.; So, J. E.; Park, S. K.; Clémancey, M.; Garcia-Serres, R.; Latour, J.-M.; Shaik, S.; Nam, W. A mononuclear non-heme iron(IV)-oxo complex which is more reactive than cytochrome P450 model compound I. *Chem. Sci.* **2011**, *2*, 1039−1045.
(47) Saouma, C. T.; Mayer, J. M. Do spin state and spin density affect hydrogen atom transfer reactivity? *Chem. Sci.* **2014**, *5*, 21−31.
(48) Usharani, D.; Lacy, D. C.; Borovik, A. S.; Shaik, S. Dichotomous Hydrogen Atom Transfer vs Proton-Coupled Electron Transfer During Activation of X−H Bonds (X = C, N, O) by Nonheme Iron−Oxo Complexes of Variable Basicity. *J. Am. Chem. Soc.* **2013**, *135*, 17090−17104.
(49) Mehn, M. P.; Fujisawa, K.; Hegg, E. L.; Que, L., Jr. Oxygen Activation by Nonheme Iron(II) Complexes: α-Keto Carboxylate versus Carboxylate. *J. Am. Chem. Soc.* **2003**, *125*, 7828−7842.
(50) Paria, S.; Que, L., Jr.; Paine, T. K. Oxidative Decarboxylation of Benzilic Acid by a Biomimetic Iron(II) Complex: Evidence for an Iron(IV)−Oxo−Hydroxo Oxidant from O_2. *Angew. Chem., Int. Ed.* **2011**, *50*, 11129−11132.
(51) Matthews, M. L.; Neumann, C. S.; Miles, L. A.; Grove, T. L.; Booker, S. J.; Krebs, C.; Walsh, C. T.; Bollinger, J. M., Jr. Substrate positioning controls the partition between halogenation and

DOI: 10.1021/acs.accounts.5b00244
Acc. Chem. Res. 2015, 48, 2443−2452

hydroxylation in the aliphatic halogenase, SyrB2. *Proc. Natl. Acad. Sci. U. S. A.* **2009**, *106*, 17723−17728.
(52) Galonić, D. P.; Barr, E. W.; Walsh, C. T.; Bollinger, J. M., Jr.; Krebs, C. Two interconverting Fe(IV) intermediates in aliphatic chlorination by the halogenase CytC3. *Nat. Chem. Biol.* **2007**, *3*, 113−116.
(53) Comba, P.; Wunderlich, S. Iron-Catalyzed Halogenation of Alkanes: Modeling of Nonheme Halogenases by Experiment and DFT Calculations. *Chem. - Eur. J.* **2010**, *16*, 7293−7299.
(54) Planas, O.; Clemancey, M.; Latour, J.-M.; Company, A.; Costas, M. Structural modeling of iron halogenases: synthesis and reactivity of halide-iron(iv)-oxo compounds. *Chem. Commun.* **2014**, *50*, 10887−10890.
(55) Chambers, M. B.; Groysman, S.; Villagran, D.; Nocera, D. G. Iron in a trigonal tris(alkoxide) ligand environment. *Inorg. Chem.* **2013**, *52*, 3159−3169.
(56) Xiao, D. J.; Bloch, E. D.; Mason, J. A.; Queen, W. L.; Matthew, R.; Hudson; Planas, N.; Borycz, J.; Dzubak, A. L.; Verma, P.; Lee, K.; Bonino, F.; Crocellà, V.; Yano, J.; Bordiga, S.; Truhlar, D. G.; Gagliardi, L.; Brown, C. M.; Long, J. R. Oxidation of ethane to ethanol by N2O in a metal−organic framework with coordinatively unsaturated iron(II) sites. *Nat. Chem.* **2014**, *6*, 590−595.
(57) Verma, P.; Vogiatzis, K. D.; Planas, N.; Borycz, J.; Xiao, D. J.; Long, J. R.; Gagliardi, L.; Truhlar, D. G. Mechanism of Oxidation of Ethane to Ethanol at Iron(IV)−Oxo Sites in Magnesium-Diluted Fe2(dobdc). *J. Am. Chem. Soc.* **2015**, *137*, 5770−5781.
(58) Hirao, H.; Ng, W. K. H.; Moeljadi, A. M. P.; Bureekaew, S. Multiscale Model for a Metal−Organic Framework: High-Spin Rebound Mechanism in the Reaction of the Oxoiron(IV) Species of Fe-MOF-74. *ACS Catal.* **2015**, *5*, 3287−3291.
(59) Ray, K.; England, J.; Fiedler, A. T.; Martinho, M.; Münck, E.; Que, L., Jr. An Inverted and More Oxidizing Isomer of $[Fe^{IV}(O)(tmc)(NCCH_3)]^{2+}$. *Angew. Chem., Int. Ed.* **2008**, *47*, 8068−8071.
(60) Kaizer, J.; Klinker, E. J.; Oh, N. Y.; Rohde, J.-U.; Song, W. J.; Stubna, A.; Kim, J.; Münck, E.; Nam, W.; Que, L., Jr. Nonheme $Fe^{IV}O$ Complexes That Can Oxidize the C-H Bonds of Cyclohexane at Room Temperature. *J. Am. Chem. Soc.* **2004**, *126*, 472−473.
(61) Xue, G.; Fiedler, A. T.; Martinho, M.; Münck, E.; Que, L., Jr. Insights into the P-to-Q Conversion in the Catalytic Cycle of Methane Monooxygenase from a Synthetic Model System. *Proc. Natl. Acad. Sci. U. S. A.* **2008**, *105*, 20615−20620.
(62) Xue, G.; Wang, D.; De Hont, R.; Fiedler, A. T.; Shan, X.; Münck, E.; Que, L., Jr. A Synthetic Precedent for the $[Fe^{IV}_2(\mu\text{-}O)_2]$ Diamond Core Proposed for Methane Monooxygenase Intermediate Q. *Proc. Natl. Acad. Sci. U. S. A.* **2007**, *104*, 20713−20718.
(63) Lim, M. H.; Rohde, J.-U.; Stubna, A.; Bukowski, M. R.; Costas, M.; Ho, R. Y. N.; Münck, E.; Nam, W.; Que, L., Jr. An Fe^{IV}═O Complex of a Tetradentate Tripodal Nonheme Ligand. *Proc. Natl. Acad. Sci. U. S. A.* **2003**, *100*, 3665−3670.
(64) Hoffart, L. M.; Barr, E. W.; Guyer, R. B.; Bollinger, J. M., Jr.; Krebs, C. Direct spectroscopic detection of a C-H-cleaving high-spin Fe(IV) complex in a prolyl-4-hydroxylase. *Proc. Natl. Acad. Sci. U. S. A.* **2006**, *103*, 14738−14743.
(65) Eser, B. E.; Barr, E. W.; Frantom, P. A.; Saleh, L.; Bollinger, J. M.; Krebs, C.; Fitzpatrick, P. F. Direct Spectroscopic Evidence for a High-Spin Fe(IV) Intermediate in Tyrosine Hydroxylase. *J. Am. Chem. Soc.* **2007**, *129*, 11334−11335.

DOI: 10.1021/acs.accounts.5b00244
Acc. Chem. Res. 2015, 48, 2443−2452